Vaccine 33 (2015) 4798–4806

Contents lists available at ScienceDirect

Vaccine

journal homepage: www.elsevier.com/locate/vaccine

A multi-trimeric fusion of CD40L and gp100 tumor antigen activates dendritic cells and enhances survival in a B16-F10 melanoma DNA vaccine model

Sachin Gupta[a], James M. Termini[a], Yaelis Rivas[a], Miguel Otero[c], Francesca N. Raffa[a], Vikas Bhat[b], Amjad Farooq[b], Geoffrey W. Stone[a,*]

[a] Department of Microbiology and Immunology, Miami Center for AIDS Research, and the Sylvester Comprehensive Cancer Center, University of Miami Miller School of Medicine, Miami, FL, USA
[b] Department of Biochemistry and Molecular Biology and the Sylvester Comprehensive Cancer Center, University of Miami Miller School of Medicine, Miami, FL, USA
[c] Department of Microbiology and Medical Zoology, University of Puerto Rico, San Juan, PR, USA

ARTICLE INFO

Article history:
Received 20 February 2015
Received in revised form 21 May 2015
Accepted 25 July 2015
Available online 1 August 2015

Keywords:
CD40L
Dendritic cell
Cancer vaccine
DNA vaccine
Surfactant protein D
B16-F10 melanoma

ABSTRACT

Vaccination with tumor-associated antigens can induce cancer-specific CD8+ T cells. A recent improvement has been the targeting of antigen to dendritic cells (DC) using antibodies that bind DC surface molecules. This study explored the use of multi-trimers of CD40L to target the gp100 melanoma tumor antigen to DC. The spontaneously-multimerizing gene Surfactant Protein D (SPD) was used to fuse gp100 tumor antigen and CD40L, creating the recombinant protein SPD-gp100-CD40L. This "third generation" DC-targeting vaccine was designed to both target antigen to DC and optimally activate dendritic cells by aggregating CD40 trimers on the DC membrane surface. SPD-gp100-CD40L expressed as a 110 kDa protein. Analytical light scattering analysis gave elution data corresponding to 4-trimer and multi-trimer SPD-gp100-CD40L oligomers. The protein was biologically active on dendritic cells and induced CD40-mediated NF-κB signaling. DNA vaccination with SPD-gp100-CD40L plasmid, together with plasmids encoding IL-12p70 and GM-CSF, significantly enhanced survival and inhibited tumor growth in a B16-F10 melanoma model. Expression of gp100 and SPD-CD40L as separate molecules did not enhance survival, highlighting the requirement to encode gp100 within SPD-CD40L for optimal vaccine activity. These data support a model where DNA vaccination with SPD-gp100-CD40L targets gp100 to DC in situ, induces activation of these DC, and generates a protective anti-tumor response when given in combination with IL-12p70 and GM-CSF plasmids.

1. Introduction

Cancer vaccination has attracted renewed attention as a therapy for the treatment of tumor growth and metastasis. The use of Tumor Associated Antigens (TAA) is particularly promising. Therapeutic effects specific to cancer cells can be generated through the careful selection of TAA preferentially expressed on tumor cells [1,2]. In particular, it has been reported that DNA vaccination using an exogenous plasmid encoding TAA can induce cancer-specific cytotoxic T lymphocytes (CTL) with antitumor activity [3,4]. However, optimal CTL activity requires that the antigen be selectively and efficiently presented by antigen presenting cells (APC). APC, including dendritic cells (DC), are critical for the initiation, programming and regulation of anti-cancer immunity [5]. One approach to increase DNA vaccine efficacy is to encode molecular adjuvants within the vaccine. Previous studies have evaluated a number of molecular adjuvants including cytokines/chemokines as well as members of the TNF superfamily of ligands [6,7]. Of particular interest is the TNFSFL molecule CD40L, the cognate ligand for CD40, which is involved in DC activation.

Abbreviations: ALS, analytical light scattering; APC, antigen presenting cell; BMDC, bone marrow derived dendritic cells; CD40L, CD40 ligand; CTL, cytotoxic T lymphocytes; DC, dendritic cell; DLS, dynamic light scattering; GM-CSF, granulocyte macrophage colony-stimulating factor; GVAX, B16-F10 cells expressing GM-CSF; IRES, internal ribosome entry site; MHC, major histocompatibility complex; M_n, number-average molar mass; M_w, weight-average molar mass; R_g, radius of gyration; R_h, hydrodynamic radius; *Ro*, Raleigh ratio; SEAP, secreted alkaline phosphatase; SLS, static light scattering; SPD, surfactant protein D; TAA, tumor associated antigen; TNFSFL, TNF superfamily ligand.

* Corresponding author. Tel.: +1 305 243-2189; fax: +1 305 243-7211.
E-mail address: gstone@med.miami.edu (G.W. Stone)

http://dx.doi.org/10.1016/j.vaccine.2015.07.081
0264-410X/

Melanoma-specific antigen gp100 is known to induce anti-gp100 immune responses and suppress melanoma tumor growth in DNA and viral vector vaccine models [8]. However, adjuvants encoded in the vaccine may further enhance the immune response to gp100. As important, targeting of tumor antigens directly to DC using the DC receptor DEC-205 has previously been shown to increase immune responses [9]. Similarly, it has also been shown that delivery of antigens to DC via CD40 can enhance cross-presentation of antigen to CD8+ T cells via MHC I [10,11].

CD40L stimulation induces the production of IL-12p70 and other cytokines by DC [12] and enhances the differentiation of effector T cells [13]. Based on previously published data [14,15] a 4-trimer secreted soluble form of CD40L has been shown to be particularly effective as a DNA vaccine adjuvant. Surfactant Protein D (SPD) was used as a scaffold to generate the 4-trimer CD40L complex. SPD is a member of the collectin family that spontaneously trimerizes and forms disulfide bonds to generate a four-trimer oligomer [16].

In addition to CD40L, other adjuvants previously tested in cancer vaccine models include GM-CSF and IL-12p70. Systemic co-administration of IL-12p70 [17] or GM-CSF [18] has been shown to induce antitumor immunity. Studies have also evaluated these cytokines as DNA-encoded adjuvants for DNA vaccines, where they have shown modest efficacy [19,20].

In the present study, a fusion protein (SPD-gp100-CD40L) was generated encoding the murine CD40L extracellular domain fused to the collagen-like domain of murine SPD, with gp100 antigen inserted within the SPD coding region. We reasoned that these soluble CD40L multi-trimers would deliver gp100 to DC while simultaneously activating the DC, thereby inducing an enhanced anti-tumor CD8+T cell response. As we report, SPD-gp100-CD40L protein was stable, formed large polymeric complexes, and was biologically active on DC, suggesting proper assembly of CD40L trimers. Co-delivery of SPD-gp100-CD40L, GM-CSF, and IL-12p70 plasmids by intramuscular injection enhanced survival of mice challenged with B16-F10 melanoma, and significantly suppressed tumor growth. This response was not observed with any other vaccine combination, and was not observed when gp100 and SPD-CD40L were delivered as separate molecules, with or without the addition of GM-CSF and IL-12p70. Overall, these data support a model whereby SPD-gp100-CD40L targets gp100 antigen to DC in situ, activates these DC via CD40 stimulation, and induces an immune response that, when augmented with GM-CSF and IL-12p70, controls tumor growth and enhances survival in a murine B16-F10 tumor model.

2. Materials and methods

2.1. Construction and preparation of DNA plasmids

Plasmid encoding human glycoprotein 100 (pgp100) was a gift of Dr. Patrick Hwu [21]. Plasmid encoding murine SPD-CD40L was generated as detailed [15]. To generate pSPD-gp100-CD40L, DNA encoding amino acids 25 to 596 (sequence KVPRNQD to EAGLGQV) of human gp100, incorporating the full extracellular domain or gp100, was inserted between amino acids 105 and 106 of mouse SPD within construct SPD-CD40L. The coding sequence was inserted between amino acid sequences GERGLSG and PPGLPGI of murine SPD. Murine IL-12p70 plasmid pIL-12 was purchased from Invivogen and encodes a single chain dimer of IL-12 p35 and p40 (InvivoGen). Murine GM-CSF plasmid was constructed using a codon-optimized gene encoding murine GM-CSF inserted into plasmid pcDNA3.1. Clone pgp100-IRES-SPD-CD40L was generated by placing an IRES sequence between human gp100 (amino acids 1-594) and murine SPD-CD40L [15]. All plasmids were propagated in *Escherichia coli* strain TOP10. DNA was initially prepared using the Giga Endofree plasmid kit (Qiagen, Inc.), followed by additional endotoxin removal with further rounds of Triton-X114 extraction [14]. All plasmid were confirmed by LAL endotoxin assay (Lonza Inc.) to be endotoxin free (<0.2 EU/ml) prior to use.

2.2. Western blot analysis

293T cells were transfected with constructs using Genjet Plus transfection reagent (Signagen Laboratories). Supernatant was collected, centrifuged and filtered 48-h later. Samples were then loaded on a 10% polyacrylamide-sodium-dodecyl sulfate gel (Bio-Rad) in the presence of DTT. Following electrophoresis, protein was blotted onto PVDF membrane (Pierce) by electrophoretic transfer, blocked, and probed with goat anti-mouse CD40L antibody (R&D Systems). For analytical light scattering analysis, supernatant following transfection of 293T cells with pSPD-gp100-CD40L was collected and concentrated 10-fold using an Amicon centrifugal filtration system with 100 kDa cutoff (Millipore).

2.3. Analytical light scattering to study hydrodynamic characterization of SPD-gp100-CD40L protein

SPD-gp100-CD40L was analyzed by Analytical Light Scattering (ALS) as described previously [22]. Briefly, a Hiload Superdex 200 size-exclusion column was used, controlled by an Akta FPLC system (GE), maintained at 10 °C in a chromatography refrigerator. Analysis was performed using a miniDAWN TREOS triple-angle static light scattering detector and QELS dynamic light scattering detector (Wyatt), coupled to an Optilab rEX differential refractive index detector (Wyatt). 293T cell supernatant of SPD-gp100-CD40L was loaded on the Superdex 200 column at 10–50 μM starting concentration. The flow rate was maintained at 1 ml/min. Data was collected using ASTRA software. Wyatt miniDAWN TREOS detector equipped with three scattering detectors positioned at 42°, 90° and 138° was employed in the flow mode, allowing resolution of the angular and concentration-dependence of static light scattering (SLS) intensity for SPD-gp100-CD40L. The QELS detector was positioned at 90° relative to the incident laser light for the resolution of time- and concentration-dependence of dynamic light scattering (DLS) intensity fluctuation. Hydrodynamic parameters associated with solution behavior of SPD-gp100-CD40L, including weighted-average molar mass (M_w), number-average molar mass (M_n), weighted-average hydrodynamic radius (R_h) and weighted-average radius of gyration (R_g) were determined using SLS data based on the Zimm model [23] and by non-linear least-squares fit of DLS data to an autocorrelation function [24]. In both the SLS and DLS measurements, protein concentration (c) along the elution profile of each protein species was determined in the ASTRA software from the change in refractive index (Δn) with respect to the solvent as measured by the Wyatt Optilab rEX detector using the following relationship: $c = (\Delta n)/(dn/dc)$ where dn/dc is the refractive index increment of the protein in solution.

2.4. CD40 SEAP assay

The ability of CD40L recombinant protein to stimulate CD40-mediated signaling was measured using a CD40-293-SEAP cell line. This reporter cell line was generated from HEK293 cells stably transfected with a plasmid expressing human CD40 and a second plasmid expressing secreted alkaline phosphatase (SEAP) under the control of NF-κB [25]. Reporter cells were plated on a 96-well plate (80,000 cells per well) and cultured with 100 μl of 293T supernatant (generated by transfection of 293T cells with CD40L recombinant expression plasmid or pcDNA3.1 control). Supernatant was added

in triplicate at various dilutions. After 18 h culture, 10 μl supernatant from each well was analyzed by incubation at 20 °C for 20 min with 100 μl QUANTI-Blue Alkaline Phosphatase reagent (InvivoGen), followed by analysis at 650 nm.

2.5. Dendritic cell generation, activation and maturation

C57BL/6 bone marrow was used to generate bone marrow derived DC (BMDC) as detailed in [26]. Briefly, bone marrow cells was isolated and washed with RPMI complete media (RPMI 1640 with 10% FBS, 50 μM Mercaptoethanol, 20 μg/ml gentamycin sulfate). Cells were then brought up in 20 ml media at 1×10^6 cells per ml and placed in a non-tissue culture treated T75 flask. A final concentration of 10 ng/ml murine recombinant IL-4 and 20 ng/ml murine recombinant GM-CSF (Peprotech, Rocky Hill, NJ) was then added. Cells were cultured at 37 °C, 5% CO_2, with media replaced on day 3. Two days later (day 5) cells were removed by gentle pipetting, counted, and added to a non-tissue culture treated 6-well plate at 1×10^6 cells/well. A total of 300 μl of either SPD-gp100-CD40L supernatant, pcDNA3.1 negative control supernatant, or Mimic positive control (15 ng/ml IL-1β, 5 ng/ml TNFα, and 1 μg/ml PGE_2) was added to each well. Cells were cultured for 36 h and then stained with maturation and activation markers. All BMDC samples were stained with Hamster anti-mouse CD11c clone N418 PE-Cyanine7 conjugate (eBioscience, San Diego, CA). Individual samples were also stained with eBioscience antibodies: anti-mouse CD80 (16-10A1), anti-mouse CD86 (GL1), anti-mouse CD83 (Michel-17), anti-mouse CCR7 (4B12), anti-mouse MHC Class II (I-A/I-E) (M5-114.15.2), or anti-mouse CD40 (1C10). Flow cytometry was performed and then analyzed using FlowJo 7.6.4. All samples were gated on CD11c + DC. A total of three independent wells were analyzed per condition.

2.6. Tumor immunotherapy studies

Female C57BL/6 mice (7–8 weeks old) were used in all experiments. Protocols were performed following national and institutional guidance for animal care and were approved by the IACUC of the University of Miami. Animals were housed at the University of Miami under NIH guidelines. All tumor immunotherapy studies included 5 mice per group. A total of 50,000 B16-F10 cells were injected i.d. into the left flank. Mice were then injected i.m. with plasmid DNA on day 3, 10, and 17 into both hind quadriceps muscles. Mice received a mixture of up to three plasmid constructs per injection. Empty vector pcDNA3.1 was used as filler to ensure all groups received the same total micrograms of plasmid. Tumor volume was measured 3 times per week using a digital caliper, measuring the longest diameter (a) and shortest width (b). Tumor volume was calculated by the formula $V\ (mm^3) = 0.5 \times ab^2$. Animals were euthanized when tumors reached >1500 mm^3. For GVAX vaccination, B16-F10 tumor cells expressing GM-CSF, kindly provided by Dr. G. Dranoff, were irradiated (5000 rad) and 1×10^6 cells were injected subcutaneously on the right flank on day 3, 6, and 9 [27].

2.7. Statistical analysis

Graph pad Prism 6.0 software was used for all analysis. One-way ANOVA was performed to determine significance, followed by a two-tailed Student's *t*-test or a Mann–Whitney *t*-test as described. A p value of 0.05 was considered significant. Survival was determined by a log-rank analysis of Kaplan–Meier survival curves. For all figures, p values are noted as $p < 0.05$ (*), $p < 0.01$ (**), or $p < 0.001$ (***).

3. Results

3.1. Construction and expression of multi-trimeric soluble SPD-gp100-CD40L

Previous studies have shown that CD40L-mediated signaling is required for functional CD8+ T cell memory development against tumors [28–30]. Similarly, we have previously shown that injection of plasmid DNA expressing SPD-CD40L into B16-F10 tumors can slow tumor growth when combined with TLR agonists [14]. CD40L mediates the co-stimulation, activation, and maturation of dendritic cells (DC), and this function is critical for the induction of an effective T cell-mediated immune response [31,32]. Previous research has shown that monoclonal antibodies targeting the DC surface protein DEC-205 can target cancer antigens to DC in vivo [33], inducing a protective immune response. We surmised that SPD-CD40L could similarly be used as a carrier to transport tumor-associated antigens (TAA) to DC in vivo by incorporating the antigen within the SPD collagen-like domain of SPD-CD40L. As proof of concept we constructed the plasmid pSPD-gp100-CD40L, where human gp100 is fused between amino acids 105 and 106 of the collagen-like domain of murine SPD-CD40L (Fig. 1a). A model of the expected 4-trimer complex is shown in Fig. 1b. Following transfection of pSPD-gp100-CD40L into 293T cells, secreted SPD-gp100-CD40L was detected at the expected size of 110 KDa by SDS-PAGE Western blot in the presence of DTT (Fig. 1c).

3.2. SPD-gp100-CD40L undergoes extensive oligomerization in solution

To determine the extent of SPD-gp100-CD40L multi-trimerization, we conducted analytical light scattering (ALS) analysis and quantified physical parameters of the protein construct in solution (Fig. 2 and Suppl. Data Table 1). SPD-gp100-CD40L elutes as a minor peak of ~1.4 MD and a major peak of ~9 MD (Fig. 2). These peaks correspond to the molecular weight of 4-trimer SPD-gp100-CD40L (~1.4 MD) and a range of higher molecular weight species (megamer) that are consistent with previous electron microscopy analysis of rat SPD [16]. The SPD-gp100-CD40L 4-trimer peak is predominantly monodispersed ($M_w/M_n = 1$), while the higher molecular weight megamer species contain a high degree of polydispersity ($M_w/M_n > 1$) (Suppl. Data Table 1). Both species appear to adopt an elongated rod-like shape ($R_g/R_h > 1$) in lieu of a more spherical or disc-like architecture, again consistent with the previously characterized molecular structure of SPD polymers [16].

3.3. Biological activity of SPD-gp100-CD40L

To confirm that SPD-gp100-CD40L retains biological activity, a secreted alkaline phosphatase (SEAP) cell line reporter assay was performed as described previously [34]. We monitored the ability of SPD-gp100-CD40L supernatant to drive NF-κB-mediated expression of the SEAP reporter enzyme on HEK293 cells expressing CD40. Empty vector pcDNA3.1 transfected 293T cell supernatant was used as a negative control. As shown in Fig. 3a, both SPD-CD40L and SPD-gp100-CD40L induced SEAP activity at a similar level in a dose-dependent manner when compared to empty vector. Next, we evaluated the ability of SPD-gp100-CD40L to activate bone marrow derived mouse DC. DC were cultured with supernatant from 293T cells transfected with either empty vector pcDNA3.1 or pSPD-gp100-CD40L. We observed a significant increase in CD80, CD86 and CD83 MFI, consistent with the ability of SPD-CD40L oligomers to induce DC activation and maturation [35].

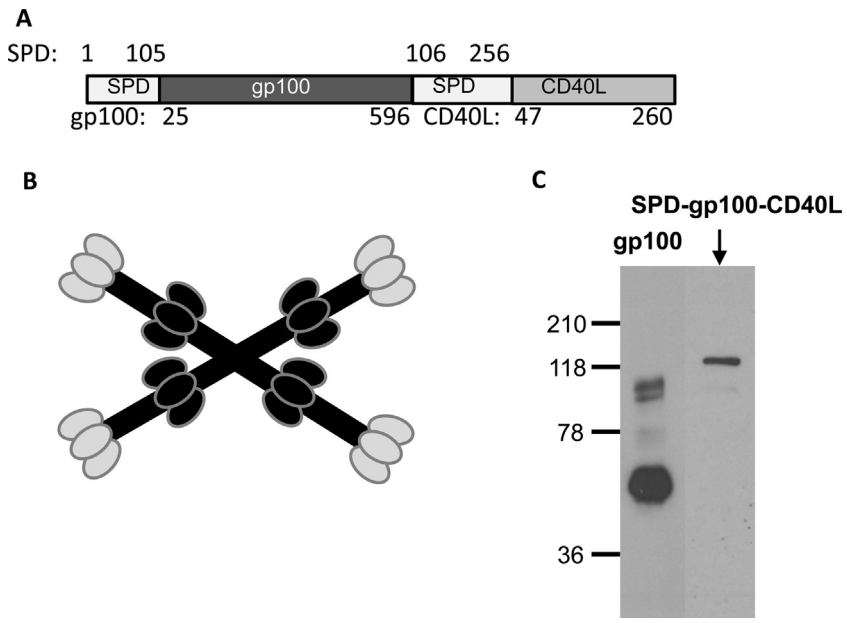

Fig. 1. Construction and Western blotting of SPD-gp100-CD40L. (a) Model of SPD-gp100-CD40L. Amino acids 25 to 596 (sequence KVPRNQD to EAGLGQV) of human gp100 were inserted between amino acids 105 and 106 of murine SPD within the SPD-CD40L fusion construct. (b) Cartoon of expected SPD-gp100-CD40L 4-trimer structure showing trimers of CD40L (gray circles) and trimers of gp100 (black circles) extending from the SPD collagen-like domain. (c) Western blot analysis. 293T cells were transfected with DNA plasmid encoding gp100 or SPD-gp100-CD40L fusion protein. After 48-hour culture, supernatant was collected and run on an SDS-PAGE gel in the presence of reducing agent. Western blot was performed using a polyclonal antibody to gp100.

3.4. SPD-gp100-CD40L DNA vaccine did not inhibit B16-F10 tumor growth in mice

We next investigated the in vivo anti-tumor activity of pSPD-gp100-CD40L plasmid, using a B16-F10 melanoma therapeutic DNA vaccination model (Fig. 4). Mice were divided into three vaccination groups: (i) PBS, (ii) pSPD-gp100-CD40L, and (iii) GVAX therapy. Group (ii) received 100 μg of pSPD-gp100-CD40L per intramuscular vaccination. We did not observe a statistical difference in tumor sizes and survival between groups (Fig. 4b and c), suggesting that pSPD-gp100-CD40L alone is insufficient to induce an anti-tumor activity. However, we observed slower tumor growth in mice treated with the "gold standard" GVAX vaccine, consistent with previous reports [27].

3.5. The combination of pSPD-gp100-CD40L, pGM-CSF, and pIL-12p70 significantly inhibited tumor growth and enhanced survival in a B16-F10 therapeutic DNA vaccine model

Next, we investigated whether SPD-gp100-CD40L treatment could be enhanced using the molecular adjuvants GM-CSF and IL-12p70. We hypothesized that DC chemo-attraction induced by GM-CSF and T cell costimulation induced by IL-12p70 would synergize with CD40L-mediated DC activation by SPD-gp100-CD40L, increasing the overall anti-tumor immune response. Mice were divided into 5 vaccination groups: (i) PBS, (ii) pSPD-gp100-CD40L + pGM-CSF, (iii) pSPD-gp100-CD40L + pIL-12, (iv) pSPD-gp100-CD40L + pGM-CSF + pIL-12, and (v) GVAX. Empty vector pcDNA3.1 was used as filler to ensure all DNA vaccine groups received the same quantity of total plasmid per vaccination (120 μg). All DNA vaccinations contained 80 μg of pSPD-gp100-CD40L and 20 μg each of pGM-CSF, pIL-12, and/or pcDNA3.1. The mean tumor size for group (iv) (SPD-gp100-CD40L + GM-CSF + IL-12) was significantly lower compared to groups (i), (ii), and (iii) on days 15, 17, and 20 (Fig. 5b). We also observed a statistically significant difference in survival between group (iv) and groups (i), (ii) and (iii) ($p < 0.05$) (Fig. 5c), and a statistically significant difference in tumor-free survival between group (iv) and groups (i), (ii), and (iii) ($p < 0.01$). As shown in Fig. 5d, five out of five mice in group (iv) were free of palpable tumors on day 11 while five out of five mice in groups (i) (ii) and (iii) had palpable tumors on day 11. The GVAX "gold standard" vaccination slowed tumor growth compared to untreated animals, however neither tumor growth nor survival reached statistical significance when comparing GVAX to other groups (Fig. 5b and c). Next, we tested various additional combinations of gp100, SPD-CD40L, GM-CSF, and IL-12. We tested gp100 plus IL-12 and/or GM-CSF, as well as a plasmid expressing gp100 and SPD-CD40L as separate molecules (gp100-IRES-SPD-CD40L) (Fig. 6a). We observed no statistical difference in mean tumor size and survival between any of the six groups and untreated mice (Fig. 6b and c). In contrast, we observed a significant delay in tumor growth and long-term survival for 4/5 mice treated with plasmid expressing SPD-gp100-CD40L + GM-CSF + IL-12.

4. Discussion

Recent advances in cancer immunotherapy support the concept that the immune system can induce antitumor responses capable of slowing tumor growth and enhancing survival [36,37]. In this context it has been reported that DNA vaccination is effective at preventing metastasis and relapse [2,4,38]. In particular, the application of DNA vaccination against melanoma has shown promise following the identification of tumor-associated antigens including gp100, MART-1 and TRP2 [39,40]. For the most part, melanoma DNA therapeutic vaccines are based on the expression of full-length antigen following intramuscular injection or electroporation of plasmid DNA. The antigen is secreted from the vaccination site and taken up by APC within the vaccine site or the local draining lymph node [41]. However, it is becoming recognized in the field that targeting cancer antigens directly to APC (in particular dendritic cells) induces a more effective immune response compared to untargeted tumor antigens [5,33,42]. We hypothesized that fusing melanoma antigen gp100 within the SPD collagen-like domain of SPD-CD40L multi-trimeric clusters [14,15] would: (1)

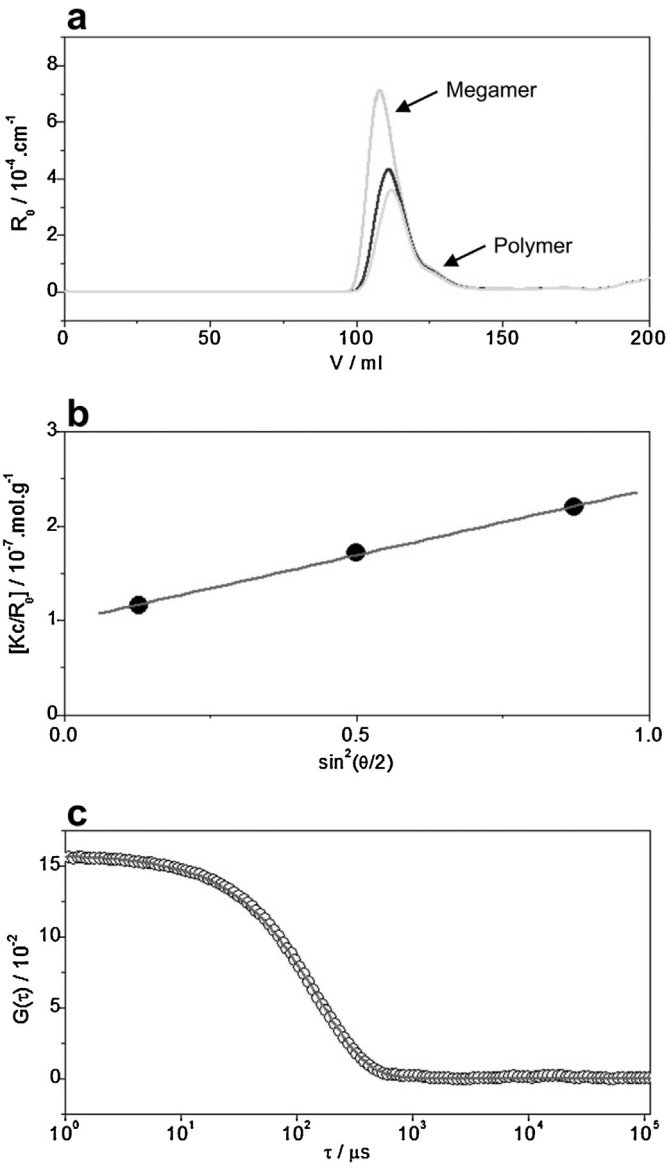

Fig. 2. Hydrodynamic analysis of SPD-gp100-CD40L. (a) Representative SEC elution profile of SPD-gp100-CD40L as monitored by the scattering intensity, expressed in terms of the excess Rayleigh ratio (R_θ), at three scattering angles of 42° (tall gray line), 90° (black line) and 138° (short gray line) as a function of elution volume (V). Note that SPD-gp100-CD40L apparently elutes as a major species (megamer) and as a minor species (polymer, evident as a shoulder of the major elution peak). (b) Representative partial Zimm plot obtained from analytical SLS measurements at a specific protein concentration for the SPD-gp100-CD40L complex. The line through the data points—collected at three scattering angles of 42°, 90° and 138°—represents a linear fit. (c) Representative autocorrelation function plot obtained from analytical DLS measurements at a specific protein concentration for the SPD-gp100-CD40L complex. The line through the data points—collected at a scattering angle of 90°—represents non-linear least squares fit.

target gp100 to DC expressing CD40 in situ, (2) induce cross presentation of gp100 by these DC, possibly via delivery of gp100 to the early endosome [10], and (3) activate and mature the DC via CD40 crosslinking with CD40L multi-trimers on the DC membrane surface [35]. We generated SPD-gp100-CD40L as a proof of concept for this approach. The SPD-gp100-CD40L fusion is a single gene of 3.1 kb that can be encoded within DNA, RNA, or viral vector cancer vaccines. Initially, we determined that SPD-gp100-CD40L was efficiently secreted from transfected cells and formed large multimeric complexes. Western blotting showed that SPD-gp100-CD40L was expressed and secreted into the culture supernatant and was of the expected molecular weight of 110 kDa. Analytical light scattering provided evidence that SPD-gp100-CD40L was forming soluble multimeric complexes, including a distinct monodispersed peak consistent with a 4-trimer complex (Fig. 2a). We also confirmed the biological activity of SPD-gp100-CD40L protein using an NF-κB reporter system and a DC activation assay. Together these data suggest that SPD-gp100-CD40L is forming a biologically active protein with a trimeric CD40L headgroup, in a manner similar to the previously characterized SPD-CD40L [15,35,43], and that these trimers are forming spontaneous 4-trimer complexes, consistent with the native SPD oligomer [16].

In an initial cancer DNA vaccine model, therapeutic immunization with pSPD-gp100-CD40L failed to control tumor growth or improve survival of mice challenged with B16-F10 melanoma (Fig. 4). This is not surprising, given the aggressive nature of B16-F10 tumors [44]. One possibility is that secretion of immunosuppressive cytokines such as VEGF, IL-10 and TGF-ß by B16-F10 prevented activated cytotoxic T lymphocytes (CTL), induced by SPD-gp100-CD40L, from entering into the tumor bed. Alternately, immunosuppressive cytokines suppressed cytotoxic activity once the CTL entered the tumor tissue [45,46]. Previous studies have evaluated cytokines IL-12 and GM-CSF for their ability to enhance T cell mediated immune responses [20]. We therefore hypothesized that SPD-gp100-CD40L combined with cytokines IL-12 and GM-CSF would both enhance antigen cross-presentation (via SPD-gp100-CD40L) and induce immune activation (via GM-CSF and IL-12), overcoming tumor-mediated immune suppression. Consistent with this hypothesis, we observed that vaccination with all 3 plasmids significantly slowed tumor growth, delayed tumor onset, and improved mouse survival (Fig. 5). In particular, SPD-gp100-CD40L + IL-12 + GM-CSF inhibited tumor growth compared to GVAX. However, we observed rapid progression of tumors after day 20 in animals given the 3 plasmids, despite the delayed tumor growth, resulting in survival of only 1/5 mice by day 35. Only the triple combination was effective, and all other combinations failed to significantly suppress tumor growth or enhance survival (Figs. 5 and 6). Comparing Figs. 5 and 6, we did observe some experimental variation in the response to SPD-gp100-CD40L + IL-12 + GM-CSF, including long term survival of 4/5 mice in Fig. 6 compared to 1/5 mice in Fig. 5. However, overall SPD-gp100-CD40L + IL-12 + GM-CSF provided superior response to alternative combinations. Expression of gp100 and SPD-CD40L as separate molecules also failed to slow tumor growth, consistent with the hypothesis that dendritic cell targeting is an important component of SPD-gp100-CD40L activity. Animals received the same total amount of plasmid per vaccination (120 μg) in all experiments, allowing us to control for immune stimulation provided by plasmid DNA itself. Based on the literature and our data, we propose a model where the effectiveness of SPD-gp100-CD40L is mediated by the targeting of gp100 to DC, enhanced cross-presentation via CD40-mediated delivery to the early endosome [10,11], and the capacity of CD40L multi-trimers to activate and mature DC [15,35]. Furthermore, IL-12-p70-mediated T cell stimulation and GM-CSF-mediated DC chemoattraction enhanced the CD8+ T cell response against SPD-gp100-CD40L, inhibiting B16-F10 tumor growth and enhancing survival. These data suggest that CD40L stimulation is a critical component of the vaccine. We did not observe reduced tumor growth when gp100 was combined with IL-12 and GM-CSF in the absence of CD40L, despite overall higher levels of gp100 protein expression in pgp100 transfected cells compared to pSPD-gp100-CD40L transfected cells (Fig. 1c). In addition, the delivery of gp100 and SPD-CD40L as separate molecules (using an IRES construct) was unable to replicate the effectiveness of SPD-gp100-CD40L (Fig. 6), consistent with the requirement that gp100 be physically linked to CD40L multi-trimers for optimal activity. Additional research will be required to determine

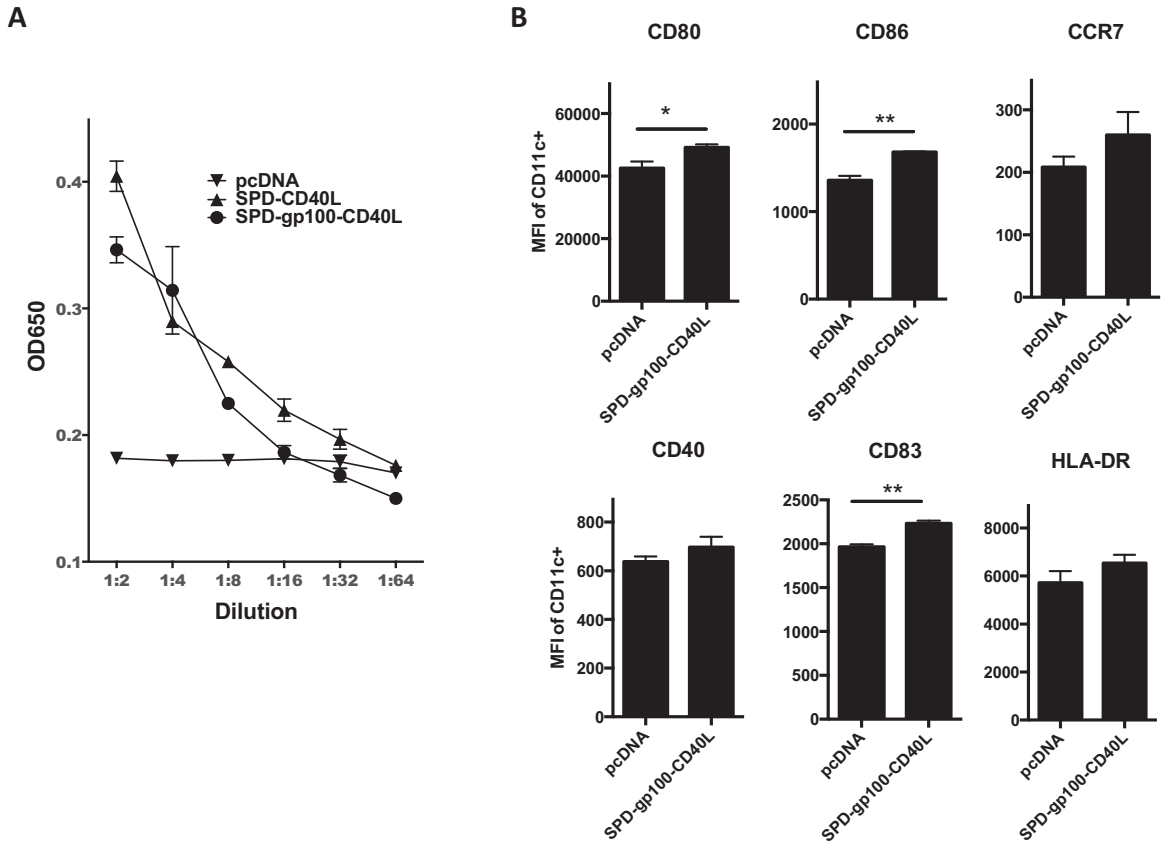

Fig. 3. Biological activity of SPD-gp100-CD40L. (a) In vitro activity of SPD-CD40L and SPD-gp100-CD40L was determined using a cell-based CD40 NF-κB enzymatic reporter system. An equivalent amount of 293T supernatant from pcDNA3.1, pSPD-CD40L or pSPD-gp100-CD40L transfected cells was incubated with 293-CD40-SEAP NF-κB reporter cells at various dilutions. (b) In vitro activity of supernatant from SPD-gp100-CD40L transfected 293T cells was evaluated on mouse bone marrow derived mouse DC and compared to supernatant from 293T cells transfected with empty vector pcDNA3.1. Error bars represent mean + SEM ($n = 3$). * $p < 0.05$, ** $p < 0.01$ by Student's t test compared to pcDNA3.1 supernatant.

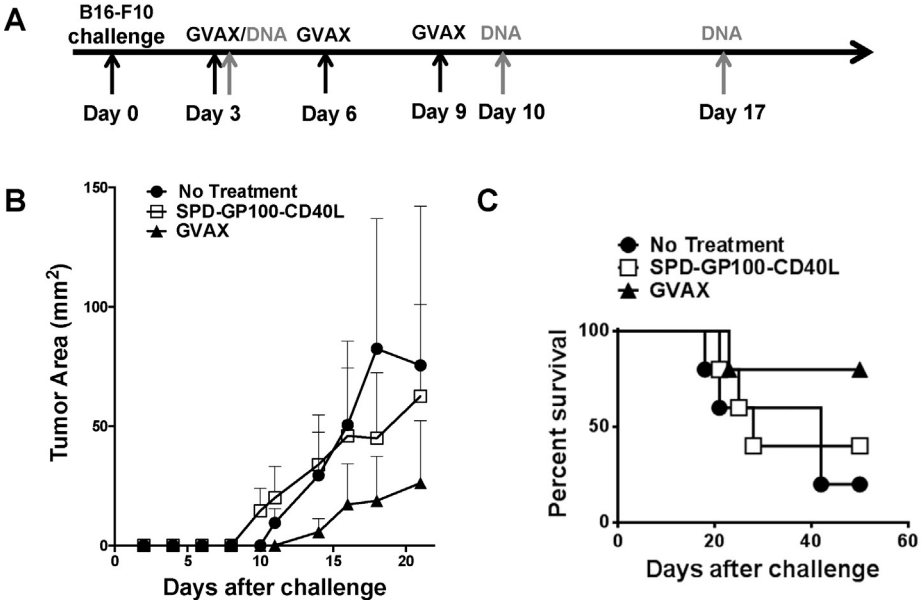

Fig. 4. B16-F10 Tumor Immunotherapy. (a) Immunization schedule for B16-F10 tumor challenge and DNA/GVAX therapeutic vaccination, as indicated by arrows. B16-F10 cells (50,000) were injected i.d. into the left flank of mice on day 0. Mice were then immunized by i.m. injection of PBS or pSPD-gp100-CD40L on day 3, 10, and 17. GVAX, B16-F10 tumor cells expressing GM-CSF, were irradiated at 5,000 rad and 1×10^6 cells injected subcutaneously on day 3, 6, and 9. (b) Tumor growth analysis. Each point represents the mean tumor volume per group ($n = 5$). (c) Survival analysis was based on the date of death or when tumor size reached >1500 cm^2.

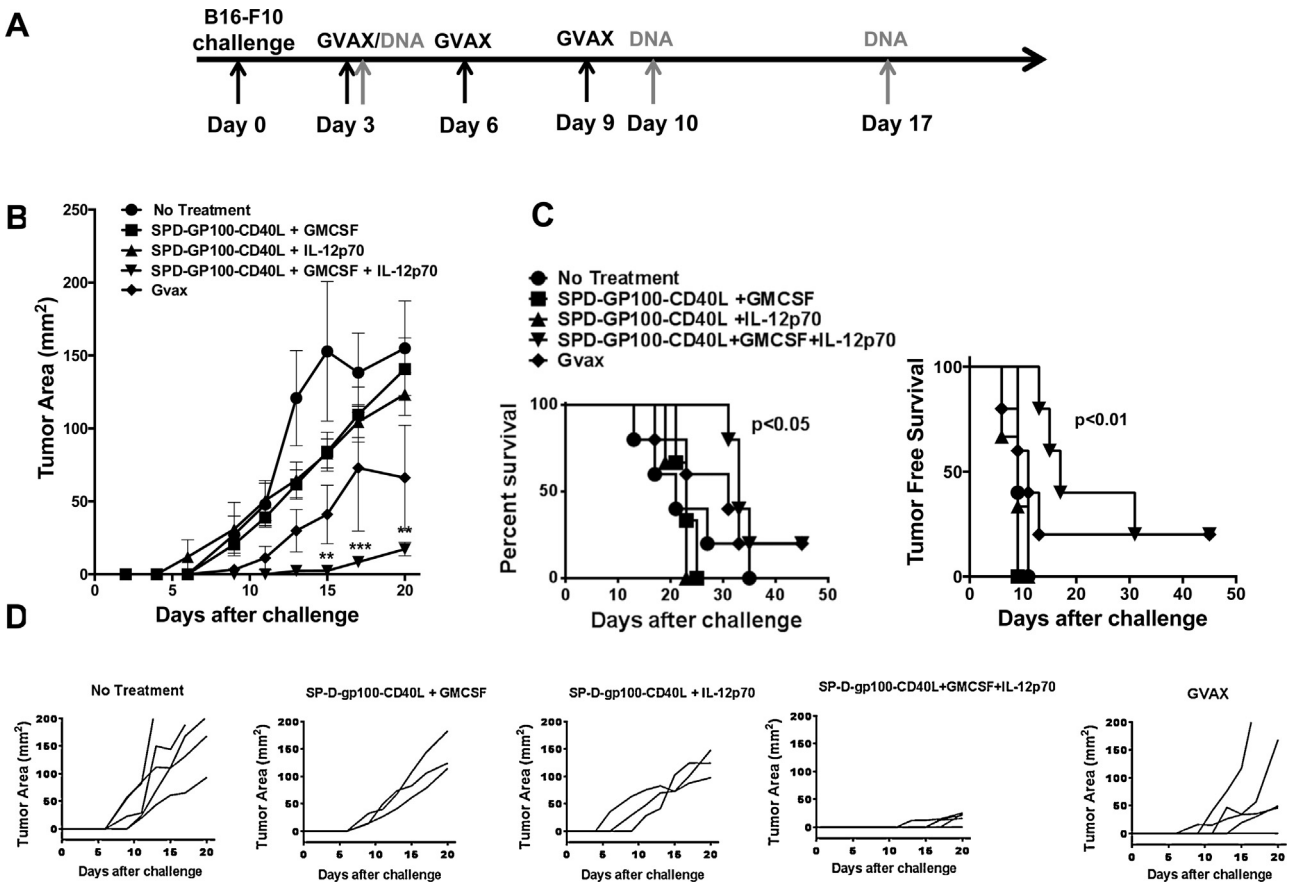

Fig. 5. DNA vaccination with a combination of pSPD-gp100-CD40L, pIL-12p70 and pGM-CSF. (a) Immunization schedule for B16-F10 tumor challenge and DNA or GVAX vaccination, as indicated by arrows. B16-F10 cells (50,000) were injected i.d. into the left flank of the mice on day 0. Mice were immunized i.m. with PBS, pSPD-gp100-CD40L + pIL-12, pSPD-gp100-CD40L + pGM-CSF, or pSPD-gp100-CD40L + pIL-12 + pGM-CSF on day 3, 10, and 17. For GVAX therapy, B16-F10 tumor cells expressing GM-CSF (GVAX), were irradiated at 5000 rad and 1×10^6 cells were injected subcutaneously on day 3, 6, and 9. (b) Tumor growth analysis. Each point represents the mean tumor volume of animals in each group ($n = 5$). (c) Survival analysis of mice. (d) Tumor growth kinetics of individual mice from each treatment arm.

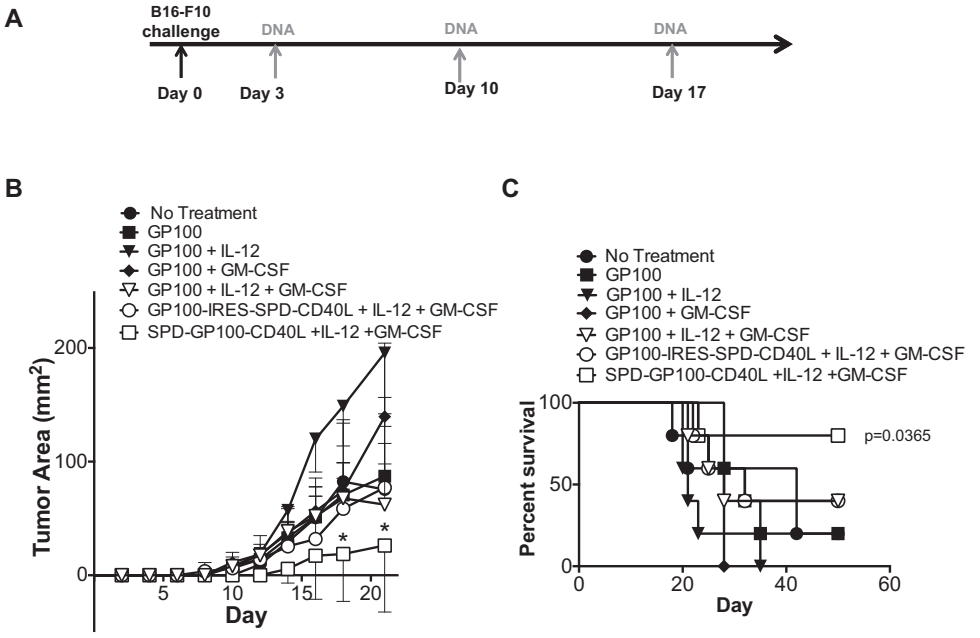

Fig. 6. Expression of gp100 and SPD-CD40L as separate proteins does not enhance anti-tumor activity. (a) Immunization schedule for B16-F10 tumor challenge and DNA vaccination, as indicated by arrows. B16-F10 cells (50,000) were injected into the left flank of the mice on day 0. Mice were then immunized i.m. with PBS, pgp100, pgp100 + pIL-12, pgp100 + pGM-CSF, pgp100 + pIL-12 + pGM-CSF, pgp100-IRES-SPD-CD40L + pIL-12 + pGM-CSF, or pSPD-gp100-CD40L + pIL-12 + pGM-CSF on day 3, 10, and 17. (b) Tumor growth analysis. Each point represents the mean tumor volume of animals in each group ($n = 5$). (c) Survival analysis of mice.

whether multi-trimerization of CD40L plays a role in the activity of this construct, however similar studies with a fusion construct expressing Gag (SPD-Gag-CD40L) showed that single trimers were not effective when compared to multi-trimer complexes [47]. Of interest, recent studies have shown that delivery of antigen using anti-CD40 agonistic antibody can enhance DC cross presentation [10,11]. Enhanced cross-presentation and the simultaneous delivery of antigen and activation of the DC may explain the unique ability of SPD-gp100-CD40L to induce a robust anti-tumor immune response.

In conclusion, this study demonstrated that encoding the gp100 tumor antigen within an SPD-CD40L DNA vaccine, combined with IL-12p70 and GM-CSF adjuvant plasmids, generates an effective antitumor response against B16-F10 melanoma. The SPD-gp100-CD40L construct is a novel DNA vaccine reagent that provides CD40-mediated APC activation in the context of efficient DC targeting and cross-presentation of cancer antigens. Future studies will explore alternative fusion proteins expressing tumor-associated antigens other than gp100. These constructs will allow us to determine whether this strategy can be expanded to a wider range of cancers. In summary, this study describes a novel reagent for use in cancer therapeutic vaccines, exploiting the unique properties of CD40L for the DC targeting, activation, and enhanced cross presentation.

Conflict of interest statement

Geoffrey Stone is listed as an inventor on patent applications related to technology described in this manuscript. All other authors have no conflict of interest.

Acknowledgements

We gratefully acknowledge Irwine Sainvil, Saravana Kanagavelu, and Kathryn A Fuller (University of Miami) for technical support and Eli Gilboa (University of Miami) and Richard Kornbluth (Multimeric Biotherapeutics, Inc.) for helpful comments. The CD40-293-SEAP cell line was kindly provided by Richard Kornbluth (Multimeric Biotherapeutics, Inc.). Human gp100 cDNA was kindly provided by Patrick Hwu (MD Anderson Cancer Center). GVAX (B16-F10 cell line expressing murine GM-CSF) was kindly provided by George Dranoff (Dana-Farber Cancer Institute). We thank Laboratory Core D of the Miami Center for AIDS Research (PI Dr. Savita Pahwa) for laboratory service support. We also thank Dr. Huw S. Kruger and staff at the University of Miami Sylvester Comprehensive Cancer Center flow cytometry core facility for flow cytometry services. This work was supported by American Cancer Society Institutional Research Grant no. 98-277-13 to the Sylvester Comprehensive Cancer Center, PI Dr. Joseph Rosenblatt (to GWS), funds from the Stanley J. Glaser Foundation (to GWS), National Institutes of Health Grant R01GM083897 (to AF), funds from the University of Miami Sylvester Braman Family Breast Cancer Institute (to AF), and NIH grant P30AI073961 to the Miami Center for AIDS Research (CFAR) at the University of Miami Miller School of Medicine.

Appendix A. Supplementary data

Supplementary data associated with this article can be found, in the online version, at http://dx.doi.org/10.1016/j.vaccine.2015.07.081

References

[1] Begley J, Ribas A. Targeted therapies to improve tumor immunotherapy. Clin Cancer Res 2008;14(Jul (14)):4385–91.
[2] Jandus C, Speiser D, Romero P. Recent advances and hurdles in melanoma immunotherapy. Pigment Cell Melanoma Res 2009;22(Dec (6)):711–23.
[3] Donnelly JJ, Wahren B, Liu MA. DNA vaccines: progress and challenges. J Immunol 2005;175(Jul (2)):633–9.
[4] Kutzler MA, Weiner DB. DNA vaccines: ready for prime time? Nat Rev Genet 2008;9(10):776–88.
[5] Melief CJ. Cancer immunotherapy by dendritic cells. Immunity 2008;29(Sep (3)):372–83.
[6] Smith CA, Farrah T, Goodwin RG, The TNF. receptor superfamily of cellular and viral proteins: activation, costimulation, and death. Cell 1994;76(Mar (6)):959–62.
[7] Abdulhaqq SA, Weiner DB. DNA vaccines: developing new strategies to enhance immune responses. Immunol Res 2008;42(1–3):219–32.
[8] Wu L, Kong WP, Nabel GJ. Enhanced breadth of CD4 T-cell immunity by DNA prime and adenovirus boost immunization to human immunodeficiency virus Env and Gag immunogens. J Virol 2005;79(Jul (13)):8024–31.
[9] Steinman RM. Dendritic cells in vivo: a key target for a new vaccine science. Immunity 2008;29(Sep (3)):319–24.
[10] Delamarre L, Holcombe H, Mellman I. Presentation of exogenous antigens on major histocompatibility complex (MHC) class I and MHC class II molecules is differentially regulated during dendritic cell maturation. J Exp Med 2003;198(Jul (1)):111–22.
[11] Chatterjee B, Smed-Sorensen A, Cohn L, Chalouni C, Vandlen R, Lee BC, et al. Internalization and endosomal degradation of receptor-bound antigens regulate the efficiency of cross presentation by human dendritic cells. Blood 2012;120(Sep (10)):2011–20.
[12] Cella M, Scheidegger D, Palmer-Lehmann K, Lane P, Lanzavecchia A, Alber G. Ligation of CD40 on dendritic cells triggers production of high levels of interleukin-12 and enhances T cell stimulatory capacity: T–T help via APC activation. J Exp Med 1996;184(2):747–52.
[13] Schoenberger SP, Toes RE, van der Voort EI, Offringa R, Melief CJ. T-cell help for cytotoxic T lymphocytes is mediated by CD40-CD40L interactions. Nature 1998;393(Jun (6684)):480–3.
[14] Stone GW, Barzee S, Snarsky V, Santucci C, Tran B, Langer R, et al. Nanoparticle-delivered multimeric soluble CD40L DNA combined with Toll-Like Receptor agonists as a treatment for melanoma. PLoS ONE 2009;4(10):e7334.
[15] Stone GW, Barzee S, Snarsky V, Kee K, Spina CA, Yu XF, et al. Multimeric soluble CD40 ligand and GITR ligand as adjuvants for human immunodeficiency virus DNA vaccines. J Virol 2006;80(Feb (4)):1762–72.
[16] Crouch E, Persson A, Chang D, Heuser J. Molecular structure of pulmonary surfactant protein D (SP-D). J Biol Chem 1994;269(25):17311–9.
[17] Rakhmilevich AL, Turner J, Ford MJ, McCabe D, Sun WH, Sondel PM, et al. Gene gun-mediated skin transfection with interleukin 12 gene results in regression of established primary and metastatic murine tumors. Proc Natl Acad Sci USA 1996;93(Jun (13)):6291–6.
[18] Jager E, Ringhoffer M, Dienes HP, Arand M, Karbach J, Jager D, et al. Granulocyte-macrophage-colony-stimulating factor enhances immune responses to melanoma-associated peptides in vivo. Int J Cancer 1996;67(Jul (1)):54–62.
[19] Chattergoon MA, Saulino V, Shames JP, Stein J, Montaner LJ, Weiner DB. Co-immunization with plasmid IL-12 generates a strong T-cell memory response in mice. Vaccine 2004;22(Apr (13–14)):1744–50.
[20] Xu R, Megati S, Roopchand V, Luckay A, Masood A, Garcia-Hand D, et al. Comparative ability of various plasmid-based cytokines and chemokines to adjuvant the activity of HIV plasmid DNA vaccines. Vaccine 2008;26(Sep (37)):4819–29.
[21] Lou Y, Wang G, Lizee G, Kim GJ, Finkelstein SE, Feng C, et al. Dendritic cells strongly boost the antitumor activity of adoptively transferred T cells in vivo. Cancer Res 2004;64(Sep (18)):6783–90.
[22] Bhat V, Olenick MB, Schuchardt BJ, Mikles DC, Deegan BJ, McDonald CB, et al. Heat-induced fibrillation of BclXL apoptotic repressor. Biophys Chem 2013;179(Sep):12–25.
[23] Wyatt PJ. Light scattering and the absolute characterization of macromolecules. Anal Chim Acta 1993;272:1–40.
[24] Chu B. Laser light scattering: basic principles and practice. Boston, MA: Academic; 1991.
[25] Maurais E, Cantin R, Tremblay MJ. Human immunodeficiency virus type 1-anchored CD40 ligand induces secretion of the chemokine interleukin-8 by human primary macrophages. Virology 2009;385(Mar (1)):227–32.
[26] Inaba K, Inaba M, Romani N, Aya H, Deguchi M, Ikehara S, et al. Generation of large numbers of dendritic cells from mouse bone marrow cultures supplemented with granulocyte/macrophage colony-stimulating factor. J Exp Med 1992;176(6):1693–702.
[27] Quezada SA, Peggs KS, Curran MA, Allison JP. CTLA4 blockade and GM-CSF combination immunotherapy alters the intratumor balance of effector and regulatory T cells. J Clin Invest 2006;116(7):1935–45.
[28] van Mierlo GJ, den Boer AT, Medema JP, van der Voort EI, Fransen MF, Offringa R, et al. CD40 stimulation leads to effective therapy of CD40(-) tumors through induction of strong systemic cytotoxic T lymphocyte immunity. Proc Natl Acad Sci USA 2002;99(Apr (8)):5561–6.
[29] French RR, Chan HT, Tutt AL, Glennie MJ. CD40 antibody evokes a cytotoxic T-cell response that eradicates lymphoma and bypasses T-cell help. Nat Med 1999;5(5):548–53.
[30] Sotomayor EM, Borrello I, Tubb E, Rattis FM, Bien H, Lu Z, et al. Conversion of tumor-specific CD4+ T-cell tolerance to T-cell priming through in vivo ligation of CD40. Nat Med 1999;5(7):780–7.
[31] Bachmann MF, Schwarz K, Wolint P, Meijerink E, Martin S, Manolova V, et al. Cutting edge: distinct roles for T help and CD40/CD40 ligand in regulating

differentiation of proliferation-competent memory CD8+ T cells. J Immunol 2004;173(Aug (4)):2217–21.
[32] Fujii S, Liu K, Smith C, Bonito AJ, Steinman RM. The linkage of innate to adaptive immunity via maturing dendritic cells in vivo requires CD40 ligation in addition to antigen presentation and CD80/86 costimulation. J Exp Med 2004;199(Jun (12)):1607–18.
[33] Bonifaz LC, Bonnyay DP, Charalambous A, Darguste DI, Fujii S, Soares H, et al. In vivo targeting of antigens to maturing dendritic cells via the DEC-205 receptor improves T cell vaccination. J Exp Med 2004;199(Mar (6)):815–24.
[34] Kanagavelu SK, Snarsky V, Termini JM, Gupta S, Barzee S, Wright JA, et al. Soluble multi-trimeric TNF superfamily ligand adjuvants enhance immune responses to a HIV-1 Gag DNA vaccine. Vaccine 2012;30(Jan (4)):691–702.
[35] Haswell LE, Glennie MJ, Al-Shamkhani A. Analysis of the oligomeric requirement for signaling by CD40 using soluble multimeric forms of its ligand CD154. Eur J Immunol 2001;31(10):3094–100.
[36] Grosso JF, Jure-Kunkel MN. CTLA-4 blockade in tumor models: an overview of preclinical and translational research. Cancer Immunol 2013;13:5.
[37] Sheikh NA, Petrylak D, Kantoff PW, Dela Rosa C, Stewart FP, Kuan LY, et al. Sipuleucel-T immune parameters correlate with survival: an analysis of the randomized phase 3 clinical trials in men with castration-resistant prostate cancer. Cancer Immunol Immunother 2013;62(1):137–47.
[38] Terando AM, Faries MB, Morton DL. Vaccine therapy for melanoma: current status and future directions. Vaccine 2007;25(Sep (Suppl. 2)):B4–16.
[39] Bloom MB, Perry-Lalley D, Robbins PF, Li Y, el-Gamil M, Rosenberg SA, et al. Identification of tyrosinase-related protein 2 as a tumor rejection antigen for the B16 melanoma. J Exp Med 1997;185(Feb (3)):453–9.
[40] de Vries TJ, Fourkour A, Wobbes T, Verkroost G, Ruiter DJ, van Muijen GN. Heterogeneous expression of immunotherapy candidate proteins gp100 MART-1, and tyrosinase in human melanoma cell lines and in human melanocytic lesions. Cancer Res 1997;57(Aug (15)):3223–9.
[41] Rice J, Ottensmeier CH, Stevenson FK. DNA vaccines: precision tools for activating effective immunity against cancer. Nat Rev Cancer 2008;8(2):108–20.
[42] Chattergoon MA, Robinson TM, Boyer JD, Weiner DB. Specific immune induction following DNA-based immunization through in vivo transfection and activation of macrophages/antigen-presenting cells. J Immunol 1998;160(Jun (12)):5707–18.
[43] Stone GW, Barzee S, Snarsky V, Spina CA, Lifson JD, Pillai VK, et al. Macaque multimeric soluble CD40 ligand and GITR ligand constructs are immunostimulatory molecules in vitro. Clin Vaccine Immunol 2006;13(11):1223–30.
[44] Fidler IJ. Biological behavior of malignant melanoma cells correlated to their survival in vivo. Cancer Res 1975;35(1):218–24.
[45] Frumento G, Piazza T, Di Carlo E, Ferrini S. Targeting tumor-related immunosuppression for cancer immunotherapy. Endocr Metab Immune Disord Drug Targets 2006;6(Sep (3)):233–7.
[46] Kim R, Emi M, Tanabe K. Functional roles of immature dendritic cells in impaired immunity of solid tumour and their targeted strategies for provoking tumour immunity. Clin Exp Immunol 2006;146(Nov (2)):189–96.
[47] Gupta S, Termini JM, Raffa FN, Williams CA, Kornbluth RS, Stone GW. Vaccination with a fusion protein that introduces HIV-1 gag antigen into a multitrimer CD40L construct results in enhanced CD8+ T cell responses and protection from viral challenge by vaccinia-gag. J Virol 2014;88(Feb (3)):1492–501.